Construction of π-Stacked Supramolecular Framework Using Triphenylene-cored Metallo-organic Cage

Journal:	*Inorganic Chemistry Frontiers*
Manuscript ID	QI-RES-10-2022-002125.R1
Article Type:	Research Article
Date Submitted by the Author:	21-Nov-2022
Complete List of Authors:	Jiang, Zhilong; orgnaic chemistry &polymer, organic chemsitry Wang, Jun; Central South University, Department of Organic and Polymer Chemistry Chen, Mingzhao; College of Chemistry and Chemical Engineering, Tang, Chaolong; Mississippi State University, Department of Physics and Astronomy Zhao, He; Central South University Dong, Qiangqiang; Central South University Yu, Weidong; Central South University, Jiang, Zhiyuan; Central South University, College of Chemistry and Chemical Engineering Chen, Bangtang; Guangzhou University Li, Xiaorui; Central South University Liu, Die; Central South University Yao, Liao-Yuan; Beijing Institute of Technology, MOE Key Laboratory of Cluster Science, School of Chemistry and Chemical Engineering; The University of Hong Kong, Department of Chemistry Liu, Hui; Central South University, School of Metallugy and Environment; Chinese National Engineering Research Center for Control & Treatment of Heavy Metal Pollution, Xie, Tingzheng; Guangzhou University, Institute of Environmental Research at Great Bay Wu, Tun; Guangzhou University Yuan, Jie; Central South University, College of Chemistry and Chemical Engineering Wang, Kun; Mississippi State University, Mississippi State 39762, USA, Department of Physics and Astronomy;Department of Chemistry Li, Yiming; Central South University Wang, Pingshan; Central South University, College of Chemistry and Chemical Engineering

ARTICLE

Received 00th January 20xx,
Accepted 00th January 20xx

DOI: 10.1039/x0xx00000x

Construction of π-Stacked Supramolecular Framework Using Triphenylene-cored Metallo-organic Cage

Zhilong Jiang,‡[a] Jun Wang,‡[a] Mingzhao Chen,*[a] Chaolong Tang,[c] He Zhao,[b] Qiangqiang Dong,[b] Weidong Yu,[b] Zhiyuan Jiang,[b] Bangtang Chen,[a] Xiaorui Li,[b] Die Liu,[b] Liao-Yuan Yao,[d] Hui Liu,[b] Tingzheng Xie,[a] Tun Wu,[a] Jie Yuan,[e] Kun Wang,[c] Yiming Li,*[b] Pingshan Wang*[a,b]

Supramolecular nanocages with inner cavities have attracted increasing attention due to their fascinating molecular aesthetics and vast potential applications. Even though a wide array of discrete supramolecular cages with precisely designed sizes and shapes have been established, the controlling assembly of higher-order supramolecular frameworks from discrete molecular entities still represents a formidable challenge. In this work, a novel metallo-organic cage **[$Zn_{12}L_4$]** was assembled based on triphenylene-cored hexapod terpyridine ligand. The Synchrotron X-Ray analysis revealed a pair of enantiomeric cages in the crystal with the flexible ligands twist clockwise or anticlockwise due to the steric hindrance in the structure. Interestingly, due to the strong π-π intermolecular interaction between triphenylene units, the hierarchical packing of sphere-like cage in the crystal was controlled as a sparse packing mode with huge channels around 3.6 nm. This research sheds light on the design of strong π-π interaction in supramolecular hierarchical packing and material science.

Introduction

Molecular nanocages with well-defined inner space have shown advanced applications in the fields of molecular recognition,[1-6] catalysis,[7-10] separation,[11-14] and so on. In the past decades, numerous three-dimensional (3D) nano-cages with various sizes and shapes were achieved using different synthetic approaches, such as hydrogen bond,[15, 16] metal-organic coordination,[17-20] dynamic covalent chemistry[21, 22] and so on. Among these nano-structures, metal-organic cages based on coordination-driven self-assembly have received a lot of attention from scientists in the past three decades due to the highly predictable nature of coordination bonds and the well designability of the organic ligand.[23-28] Benefiting from their well-designed inner cavities, such metallo-cages have found useful applications in chemical sensing,[29-31] catalysis,[32-35] drug delivery[36-38] and host-guest chemistry.[39-42] Because of these advanced functional applications, chemists pay much attention to the construction of supramolecular cages with unique three-dimensional structures.

The hierarchical superstructures that comprised of discrete molecular entities is expected to yield solubility-enhanced molecular porous materials different from metal-organic frameworks (MOFs).[43] Even though a wide array of discrete supramolecular cages with precisely designed sizes and shapes have been established, the controlling assembly of higher-order supramolecular frameworks from discrete molecular entities still represents a formidable challenge. Approaches for assembled cages into porous frameworks through the supramolecular interactions to achieve better application performances are still unusual. Weak noncovalent interactions (such as metal coordination, multiple hydrogen bonding, host−guest interactions and aromatic stacking) have been employed

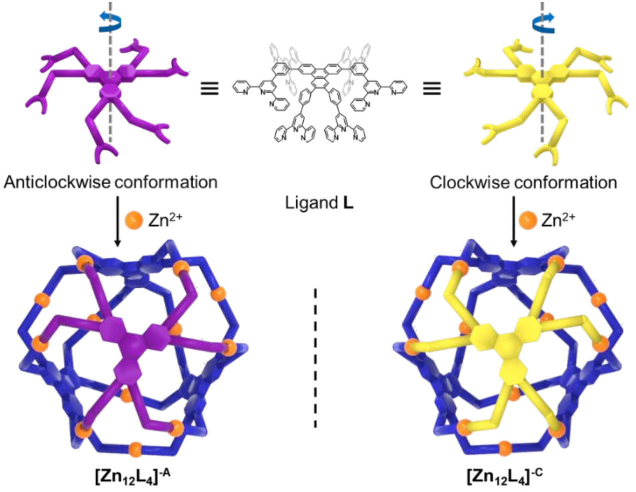

Scheme 1 Self-assembly of enantiomeric chiral metallo-organic cages **$[Zn_{12}L_4]^{-A}$** and **$[Zn_{12}L_4]^{-C}$**.

---

[a] Institute of Environmental Research at Greater Bay Area; Guangzhou Key Laboratory for Clean Energy and Materials; Key Laboratory for Water Quality and Conservation of the Pearl River Delta, Ministry of Education, Guangzhou University, Guangzhou, 510006, Guangdong, China. E-mail: jinyulinzhao@foxmail.com, chemwps@csu.edu.cn

[b] College of Chemistry and Chemical Engineering; School of Metallurgy and Environment, Central South University, Changsha, 410083, Hunan, China. E-mail: chemyl@csu.edu.cn

[c] Department of Physics Astronomy; Department of Chemistry, Mississippi State University, Mississippi State, MS 39762, USA

[d] MOE Key Laboratory of Cluster Science; School of Chemistry and Chemical Engineering, Beijing Institute of Technology, Beijing, 102488, Beijing

[e] School of Chemistry and Chemical Engineering, Henan Normal University, Xinxiang, 453007, Henan

Electronic Supplementary Information (ESI) available: Synthetic procedures, NMR spectra, ESI-MS spectra and SCXRD data, and supporting figures and table. See DOI: 10.1039/x0xx00000x

‡ These authors contributed equally to this work.

as major driving forces in intermolecular chemistry.[44-46] The π-stacking interaction is even more important to control the orientation of hierarchical assembly into higher-order architectures.

In this work, we report the self-assembly of a pair of enantiomeric metallo-organic cages by employing a C_{3v} symmetric hexapod ligand. In order to control the higher-order superstructural packing of the cage, triphenylene, one of large aromatic molecules, with extensive π-systems was introduced into the ligand as the core. Tridentate terpyridine (tpy) motifs were used as the connection units towards metals due to their extraordinary coordination ability and stability with most transition metal ions and achievements in constructing numerous supramolecular architectures.[47-49] After coordinating with Zn^{2+} ions, the hexapod building blocks lost their σ_v mirror symmetry during the formation of the supramolecule, and a twisted truncated tetrahedral cage **$[Zn_{12}L_4]$** was obtained. The single crystal X-ray diffraction of **$[Zn_{12}L_4]$** revealed that due to the steric hindrance between adjacent coordination junctions in the cage, the flexible ligands twist clockwise or anti-clockwise and generate a pair of enantiomers **$[Zn_{12}L_4]^{-A}$** and **$[Zn_{12}L_4]^{-C}$** (Scheme 1). Controlling by the π-π stacking between triphenylene units, the hierarchical packing of the supramolecular cages exhibited large triple helix channels with 3.6 nm diameter, which can be classified as 3(1,1,2) with the nomenclature of parastichy. The introduction of such fused ring molecules to induce supramolecular cage stacking is of great significance for the construction of porous frame structures, as well as in host-guest chemistry, resolution and other fields.

Results and discussion

Self-assembly and characterization of metallo-organic cage

C_{3v} symmetric hexapod ligand **L** was synthesized through a 6-fold Suzuki coupling reaction on 2,3,6,7,10,11-hexabromotriphenylene. The supramolecular cage was formed by treating ligand **L** with 3 equivalents of $Zn(NO_3)_2 \cdot 6H_2O$ in $CHCl_3$/MeOH. After precipitating with excess amount of NH_4PF_6, metallo-organic cage **$[Zn_{12}L_4]$** was obtained as a pale yellow solid in nearly quantitative yield.

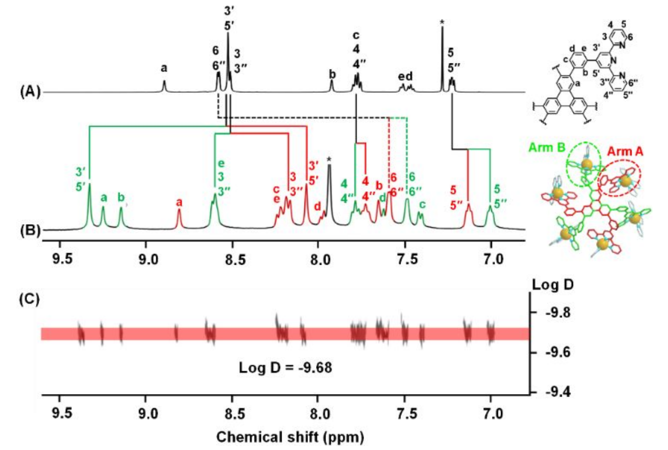

Fig. 1 (A) ^1H NMR spectrum of ligand **L** in $CDCl_3$. (B) ^1H NMR spectrum of **$[Zn_{12}L_4]$** in DMF/CD_3CN. (C) 2D DOSY spectrum of **$[Zn_{12}L_4]$** in DMF/CD_3CN.

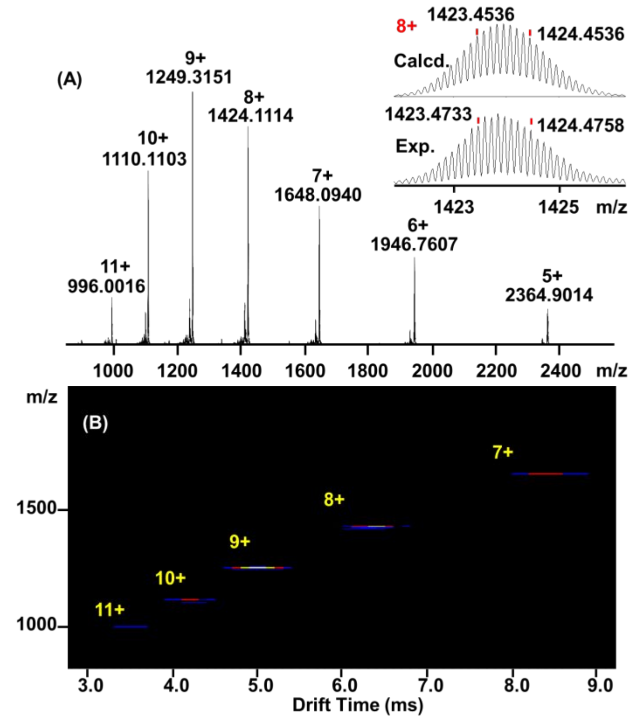

Fig. 2 (A) ESI-MS spectrum of **$[Zn_{12}L_4]$**. (B) TWIM-MS plot of **$[Zn_{12}L_4]$**.

NMR spectroscopy was first used to confirm the synthesis of supramolecular cage **$[Zn_{12}L_4]$**. From the ^1H NMR spectrum of ligand **L** in Fig. 1A, only one set of characteristic tpy-unit peaks were observed, indicating the same chemical environment of all six tpy arms and the high symmetry of the ligand. Interestingly, after the coordination, two sets of tpy-unit signals appeared in the aromatic region of **$[Zn_{12}L_4]$** (Fig. 1B). The result suggested that by forming the cage structure, the symmetry of the ligand was decreased due to the limit of arm rotation and the twist of the ligand, leading to the difference of the tpy chemical environments and the split of the signals. All of the signal peaks were fully assigned under the assistance of homonuclear chemical shift correlation spectroscopy (COSY) and nuclear overhauser effect spectroscopy (NOESY). Comparing to the ^1H NMR spectrum of **L**, the characteristic peaks of tpy-$H^{6,6''}$ in the supramolecule shifted and split from 8.59 ppm to 7.60, and 7.49 ppm due to the electron shielding effects, indicating the coordination of terpyridine units with Zn^{2+} ions. Very uncommonly, the singlet of tpy-$H^{3',5'}$ protons at 8.53 ppm were split into two singlets at 9.33 (down field shift), and 8.07 ppm (up field shift) with an integration ratio of 1:1. From the NOESY spectrum, spatial correlations were observed between the two adjacent terpyridine arms on the same benzene ring, such as A-H^c with B-H^b and B-H^c, A-tpy-$H^{3',5'}$ with B-tpy-$H^{3,3''}$, respectively (Fig. S8). Such correlations explained the unusual chemical shift caused by the electron shielding effects of spatially adjacent aromatic rings in the condensed structure[50, 51]. In addition, the signals substantiated that these two sets of signal peaks belonged to one supramolecular structure.

Moreover, diffusion-ordered spectroscopy (DOSY) was used to further confirm the component singleness of assembled product. In Fig. 1C, the spectrum exhibited a narrow band at log D= -9.68 corresponding to the ^1H NMR spectrum (Fig. 1B), further indicating that only solely composition in the self-

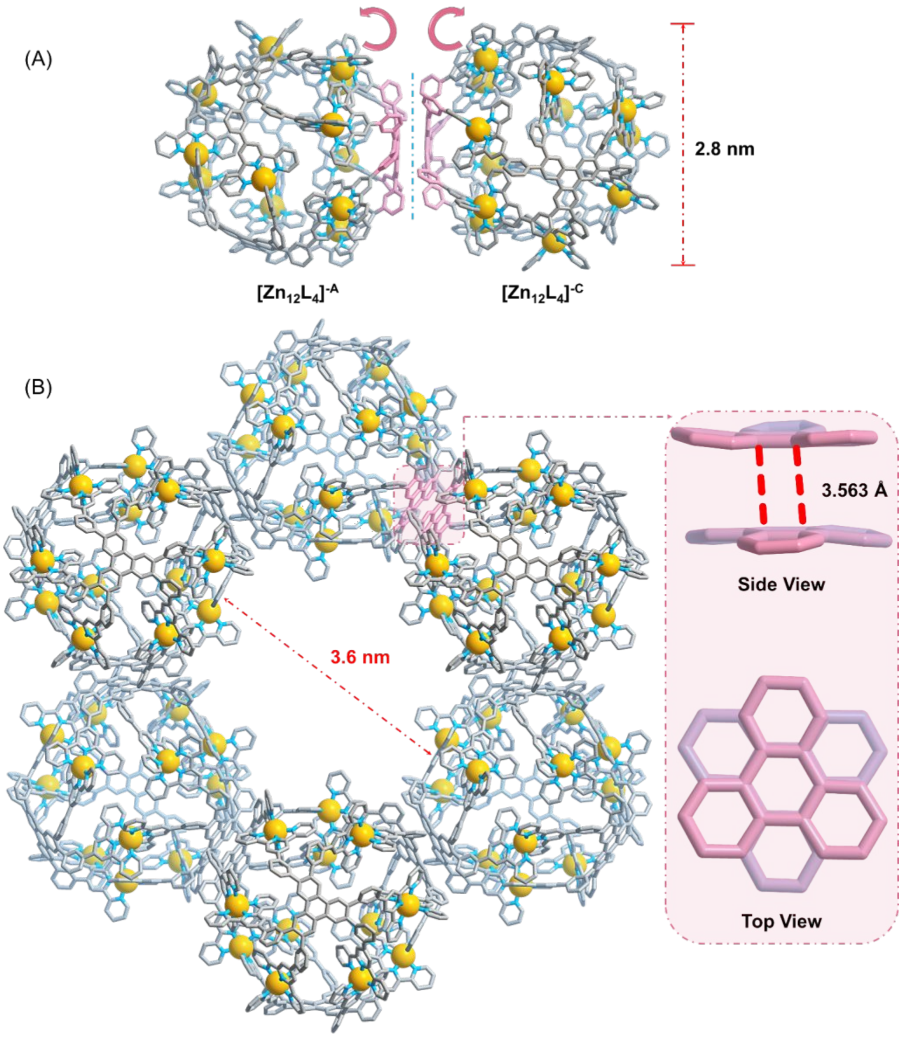

Fig. 3 (A) Crystal structure of enantiomeric supramolecular cages $\mathbf{[Zn_{12}L_4]^{-A}}$ and $\mathbf{[Zn_{12}L_4]^{-C}}$. (B) π-stacked supramolecular framework based on the π-π intermolecular interaction between triphenylene units.

assembly process. Based on the Stokes-Einstein Equation, the hydrodynamic radius (r_H) was calculated as 1.4 nm (as shown in Fig. S11), which also agreed well with the radius measured in single crystal structure.

To further investigate the composition of the assembled product, the supramolecule was tested by electrospray ionization mass spectrometry (ESI-MS) and traveling wave ion mobility mass spectrometry (TWIM-MS) experiments. The ESI-MS spectrum of $\mathbf{[Zn_{12}L_4]}$ revealed a series of peaks at m/z = 996.00, 1110.11, 1249.31, 1424.11, 1648.09, 1946.76, and 2364.90 corresponding to the continuous charge states from 11+ to 5+ due to the successive loss of PF_6^- counterions (Fig. 2A). After deconvolution, the molecular weight of the metallo-organic cage $\mathbf{[Zn_{12}L_4]}$ was calculated as 12,529 Da, which revealed the composition of $\mathbf{[Zn_{12}L_4]^{24+}}$ with 24 PF_6^- as anions. In addition, the experimental isotopic patterns of all charge states agreed well with corresponding theoretically calculated values of $\mathbf{[Zn_{12}L_4]}$ (the results can be found in Fig. S14). Furthermore, the TWIM-MS plot of $\mathbf{[Zn_{12}L_4]}$ showed a narrow drift time at charge states from 11+ to 7+, further indicating the absence of other supramolecular structures (Fig. 2B).

On account of the strong affinity between triphenylene and fullerenes through π-π stacking, C60 was selected to investigate the host-guest chemistry of the supramolecular cage. The encapsulation of fullerene occurs upon mixing C60 simultaneously with the metallo-organic cage $\mathbf{[Zn_{12}L_4]}$ in DMF/CH_3CN, followed by heating at 90 °C for 24 h. The ESI-MS revealed a series of continuous signal peaks of host-

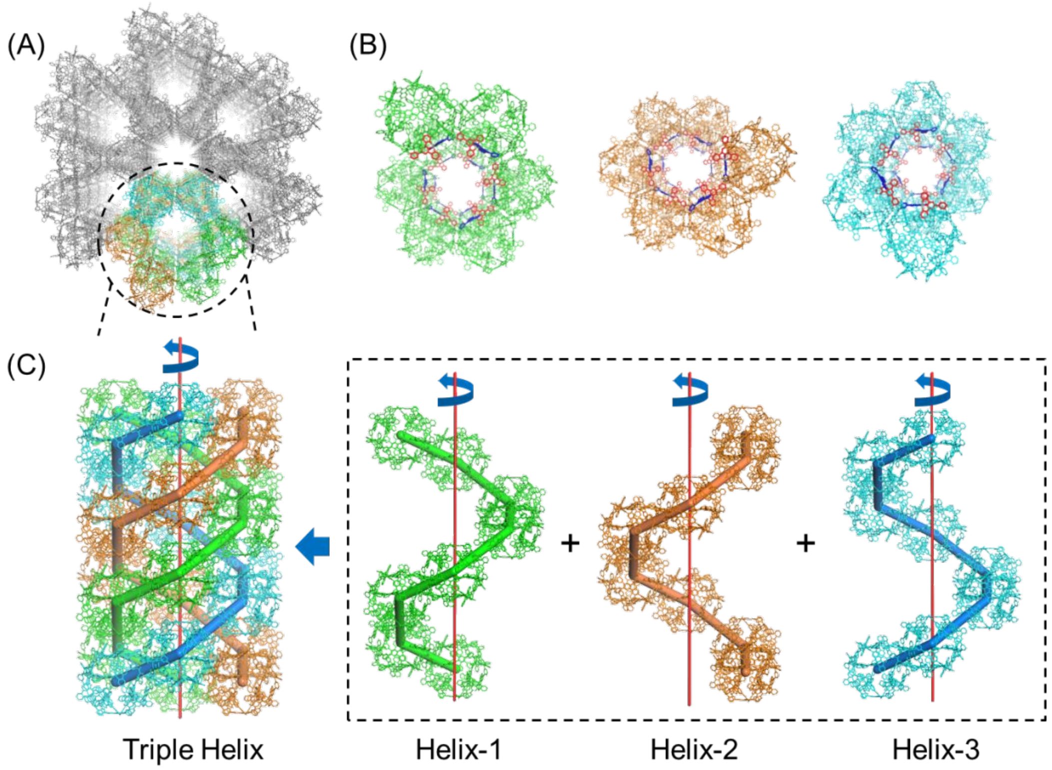

Fig. 4 (A) 3D packing analysis of metallo-organic cages. (B) top view of three helix in perspective projection. (C) Triple helix structure formed by intertwining of three complementary helices.

guest molecule C60 ⊂ **[$Zn_{12}L_4$]**, indicating the successful encapsulation of the guest molecule C60 in the supramolecular cage **[$Zn_{12}L_4$]** (Fig. S20).

Crystal structure of [$Zn_{12}L_4$]

To ambiguously reveal the structure of assembled supramolecule, single crystal X-ray diffraction was tested using the synchrotron source. However, it is extremely difficult to grow single crystals with suitable quality in 3D nanocages based on terpyridine self-assembly. Hitherto, only four crystal structures of terpyridine-based nanocages have been reported.[52-55] Fortunately, the crystal of **[$Zn_{12}L_4$]** was achieved through slow evaporation of ethyl acetate into the solution of **[$Zn_{12}L_4$]** in DMF at a constant temperature of 298 K (Fig. S22). Crystal structure revealed that the supramolecule **[$Zn_{12}L_4$]** adopts a truncated tetrahedron-like shape with a decreased T_d symmetry, composed of four triangle faces and six ship-type dimer faces. The triangle faces were formed by the connection of terpyridines on ortho-position of the same benzene, while the ship-type dimer faces were formed by the connection of the terpyridines on spaced benzene rings. Interestingly, in the same unit cell, a pair of enantiomeric cages were discovered with the hexapod ligand twisted clockwise (named as **[$Zn_{12}L_4$]$^{-C}$**) or anticlockwise (named as **[$Zn_{12}L_4$]$^{-A}$**) (Fig. 3A). It is worth noting that, the chirality of the structures was on account of the symmetry breaking caused by the configuration difference of the ligand. The ideal truncated tetrahedron belongs to T_d point group symmetry with one C_3 symmetric axis and three mirror planes across the center of the triangle face. However, in such ideal structure, the ship-type dimmer faces would have to overcome a large steric hindrance between the two swollen <tpy-Zn^{2+}-tpy> junctions. Thus, to sustain the cage structure with less steric hindrance, these two adjacent <tpy-Zn^{2+}-tpy> units adopt a staggered position and cause the twist of the ligand, leading to the loss of mirror planes and the formation of two heterochiral enantiomers. In order to isolate those enantiomeric structures, many attempts have been tried. However, not like the chiral organic cages which could be isolated by chiral HPLC, the separation of them was not successful probably due to the reversibility of the coordination bonds and the high polarity of the metallo-cages.

3D packing analysis of cage [$Zn_{12}L_4$]

In many spherical cage systems, the hierarchical packings in the crystal are usually compact as the sphere closest packing (face-centred cubic) without any large interspace. In the crystal of **[$Zn_{12}L_4$]**, strong intermolecular π-π stacking interactions between

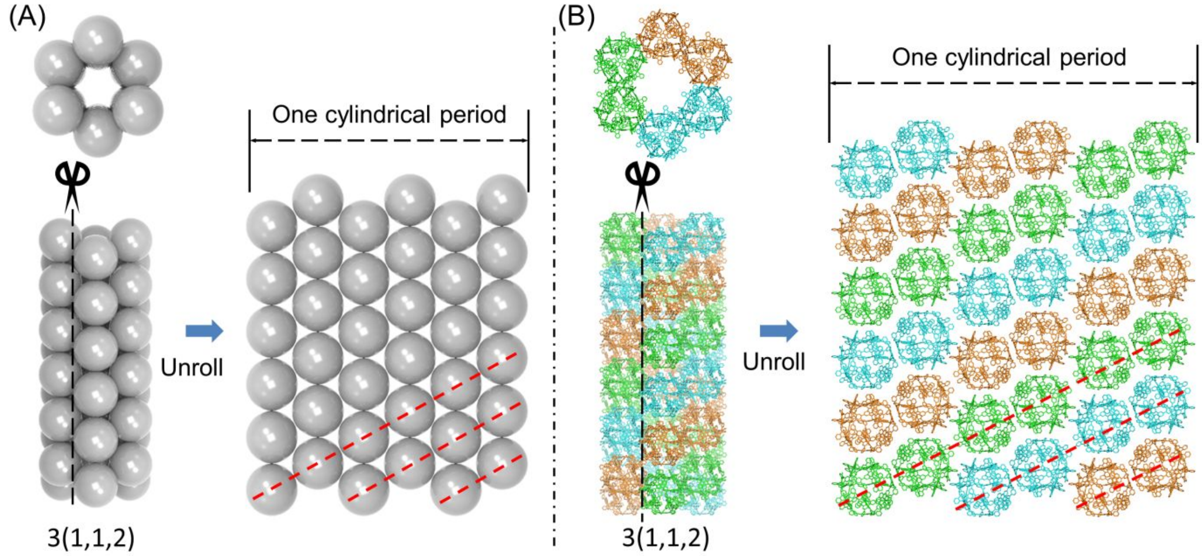

Fig. 5 Comparison of helical arrangement of sphere models and metallo-organic cage **[$Zn_{12}L_4$]**. (A) Helical arrangement of isotropic spheres with parastichy pattern 3(1,1,2), which can be unrolled along the columnar axis into the topological plane on the right. (B) Helical packing of metallo-organic cages around the channels in the crystal structure.

triphenylene planes at the truncated vertices of the cage was observed, the two triphenylene is at a distance of 3.5 Å and interlaced with a 60° angle (Fig. 3B). Interestingly, benefiting from the π-π intermolecular interaction, such sphere-like cage formed a sparse packing mode with huge channels around 3.6 nm (Fig. 4A). With such columnar cavities, this type of superstructural framework may have potential application in the fields of electronics,[56, 57] catalysis,[58, 59] energy storage,[60, 61] separation[62-64] and so on.[65, 66] Through careful observation, we found that the prominent tpy coordination junctions around the channels are not mirror symmetric, but exhibited anti-clockwise or clockwise patterns (Fig. S25) from different view. To illustrate the detailed structure, the tpy unit vertical to the channel was colored as red, and the tpy parallel to the channel was colored as blue (Fig. 4B). From the top view, the red tpy can be regarded as the arrowhead and the blue tpy as the arrow shaft. By extracting the cages upwards along the arrow direction, three helices are present in each superstructural channel (Fig. 4C), and forming an intertwined complementary triple helix structure, which is similar to the collagen structure in biological systems.[67, 68]

Furthermore, the triple helix packing of the metallo-organic cage **[$Zn_{12}L_4$]** can be classified as 3(1,1,2) according to the nomenclature of natural parastichy, which is the spiral arrangement of leaves or scales in biological systems.[69, 70] By simplifying the helical element with isotropic spheres, parastichy pattern of 3(1,1,2) was shown in Fig. 5A. To illustrate the helical arrangement and retain the symmetry of the pattern, the column was unrolled along the screw axis into a plane. In this plane, all of the spheres can be stringed with three red dashed lines, indicating the feature of triple helix structure. By unrolling the superstructural channel in the crystal of **[$Zn_{12}L_4$]**, the metallo-organic cage exhibited exactly the same pattern from the packing of parastichy 3(1,1,2) and raveled natural parastichy structure.

For the cage enantiomers, the hierarchical packing revealed that the two enantiomeric cages are coexisting in the crystal structure with 1:1 ratio, and aligning alternately into a "Kagome" topology pattern (Fig. S27B).[71, 72] In the same layer, each truncated tetrahedral cage contact with other three upside-down enantiomeric cages through the triangular faces. From the side view in Fig. S27C, enantiomers **[$Zn_{12}L_4$]$^{-C}$** and **[$Zn_{12}L_4$]$^{-A}$** are arrayed in separate straight lines with different enantiomers in the opposite directions. In these packing lines, each truncated tetrahedron contact with the upper or lower one by contacting the triangle faces towards the hexagon ones. As shown in Fig. S26E, one of the four triphenylene planes in the cage has no π-π stacking with other ones but simply faces the hollow center of the coordination triangle formed by the neighboring cage in the same packing line.

AFM and STM of cage [$Zn_{12}L_4$]

To obtain more detailed information about the metallo-organic cage **[$Zn_{12}L_4$]**, atomic force microscopy (AFM) and scanning tunneling microscopy (STM) were applied to visualize the supramolecules directly. In STM, a linear packing structure was observed on the surface of highly oriented pyrolytic graphite (HOPG). We speculated that such superstructure was attributed to the π−π interactions between the triphenylene of supramolecule **[$Zn_{12}L_4$]** and the HOPG

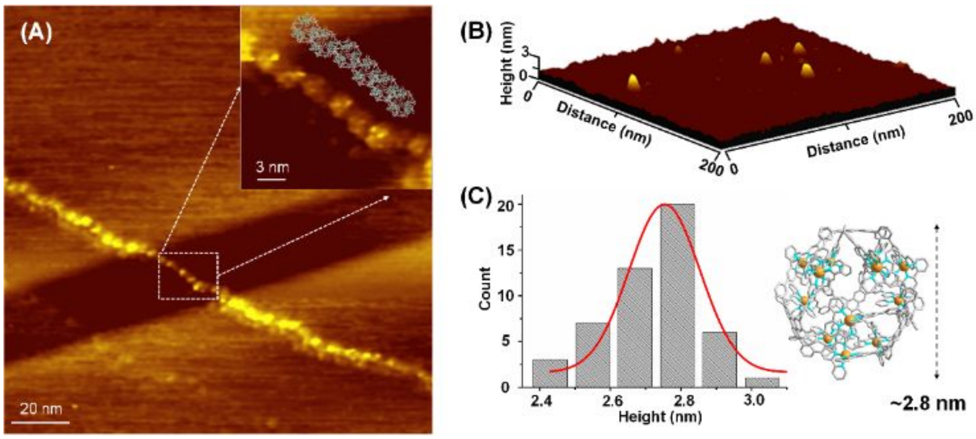

Fig. 6 STM and AFM of metallo-organic cage **[Zn$_{12}$L$_4$]**. (A) STM images of fiber-like nanostructure on a HOPG surface. (B) AFM images of metallo-organic cage **[Zn$_{12}$L$_4$]**. (C) Statistical histogram of AFM for 50 particles

surface, as well as the π−π stacking and Van der Waals' interaction between cages (Fig. 6A). The AFM images were performed by dropping a diluted DMF solution of **[Zn$_{12}$L$_4$]** (4×10^{-5} M) onto a fresh cleaved mica surface. In Fig. 6B, discrete particles were clearly observed with similar diameters. 50 dots, in total, were counted and the size distribution was shown in Fig. 6C. The result showed that most of the particles exhibited a height around 2.8 nm, which perfectly matched the size of the target supramolecular cage.

Conclusions

In summary, we have synthesized a pair of enantiomeric metallo-organic cages by employing an achiral hexapod ligand with high C_{3v} symmetry. The single crystal X-Ray diffraction revealed that due to the steric hindrance between adjacent <tpy-Zn^{2+}-tpy> connections, all of the faces in the structure twist either clockwise or anticlockwise and generate a pair of enantiomers **[Zn$_{12}$L$_4$]$^{-C}$** and **[Zn$_{12}$L$_4$]$^{-A}$**. Benefiting from the strong π-π intermolecular interaction between triphenylene units, the hierarchical packing of sphere-like cage in the crystal was controlled as a sparse packing mode with huge channels around 3.6 nm. And such channels revealed triple helix structures which showed exactly same pattern with the natural parastichy 3(1,1,2). This research not only allows the use of steric hindrance to construct chiral supramolecular cages, but also shed light on the design of strong π-π interaction in supramolecular hierarchical packing and material science.

Author Contributions

Z.J. and P.W. designed the experiments. Z.J. and J.W. completed the synthesis. B.C., H.Z. and Q.D. analyzed the NMR experimental data; M.C. and Z.J. performed MS characterization. T.X., T.W. and W.L. contributed to X-ray data collection; L.Y. and W.Y. contributed to crystallographic analysis. C.T. and K.W. contributed to AFM and STM tests; Z.J., J.W., M.C. and Y.L. analyzed the data and wrote the manuscript. P.W., M.C., D.L., H.L. and X.L. revised and supervised the manuscript. All the authors discussed the results and commented and proofread the manuscript.

Conflicts of interest

There are no conflicts to declare.

Acknowledgements

We acknowledge the support from National Natural Science Foundation of China (21971257, 22101060, 22101302) and Hunan Provincial Science and Technology Plan Project of China (No. 2019TP1001), the Excellent Youth Funding of Hunan Provincial Science and Technology Department (2022JJ20053), the Science and Technology Research Project of Guangzhou (202201020201; 202102010432). K. Wang acknowledge support from the U.S. National Science Foundation (OIA-1757220). We thank the staffs from BL17B beamline of National Facility for Protein Science Shanghai (NFPS) at Shanghai Synchrotron Radiation Facility for assistance during data collection.

References

1. M. Yamashina, Y. Tanaka, R. Lavendomme, T. K. Ronson, M. Pittelkow and J. R. Nitschke, An antiaromatic-walled nanospace, *Nature*, 2019, **574**, 511-515.
2. S. Hasegawa and G. H. Clever, Metallo-supramolecular Shell

Enables Regioselective Multi-functionalization of Fullerenes, *Chem*, 2020, **6**, 5-7.

3. Y. Wang, Y. Zhang, Z. Zhou, R. T. Vanderlinden, B. Li, B. Song, X. Li, L. Cui, J. Li, X. Jia, J. Fang, C. Li and P. J. Stang, A cyclic bis[2]catenane metallacage, *Nat. Commun.*, 2020, **11**, 2727.
4. H. Duan, Y. Li, Q. Li, P. Wang, X. Liu, L. Cheng, Y. Yu and L. Cao, Host–Guest Recognition and Fluorescence of a Tetraphenylethene-Based Octacationic Cage, *Angew. Chem. Int. Ed.*, 2020, **59**, 10101-10110.
5. H. Takezawa, R. Tabuchi, H. Sunohara and M. Fujita, Confinement of Water-Soluble Cationic Substrates in a Cationic Molecular Cage by Capping the Portals with Tripodal Anions, *J. Am. Chem. Soc.*, 2020, **142**, 17919-17922.
6. Y. Chen, G. Wu, B. Chen, H. Qu, T. Jiao, Y. Li, C. Ge, C. Zhang, L. Liang, X. Zeng, X. Cao, Q. Wang and H. Li, Self-Assembly of a Purely Covalent Cage with Homochirality by Imine Formation in Water, *Angew. Chem. Int. Ed.*, 2021, **60**, 18815-18820.
7. Z. Zhou, J. Liu, J. Huang, T. W. Rees, Y. Wang, H. Wang, X. Li, H. Chao and P. J. Stang, A self-assembled Ru-Pt metallacage as a lysosome-targeting photosensitizer for 2-photon photodynamic therapy, *Proc. Natl. Acad. Sci. U S A*, 2019, **116**, 20296-20302.
8. W. Cullen, H. Takezawa and M. Fujita, Demethylenation of Cyclopropanes via Photoinduced Guest-to-Host Electron Transfer in an M_6L_4 Cage, *Angew. Chem. Int. Ed.*, 2019, **58**, 9171-9173.
9. T. A. Bender, R. G. Bergman, K. N. Raymond and F. D. Toste, A Supramolecular Strategy for Selective Catalytic Hydrogenation Independent of Remote Chain Length, *J. Am. Chem. Soc.*, 2019, **141**, 11806-11810.
10. K. Omoto, S. Tashiro and M. Shionoya, Phase-Dependent Reactivity and Host–Guest Behaviors of a Metallo-Macrocycle in Liquid and Solid-State Photosensitized Oxygenation Reactions, *J. Am. Chem. Soc.*, 2021, **143**, 5406-5412.
11. L. Ma, C. J. E. Haynes, A. B. Grommet, A. Walczak, C. C. Parkins, C. M. Doherty, L. Longley, A. Tron, A. R. Stefankiewicz, T. D. Bennett and J. R. Nitschke, Coordination cages as permanently porous ionic liquids, *Nat. Chem.*, 2020, **12**, 270-275.
12. H. Zeng, M. Xie, T. Wang, R.-J. Wei, X.-J. Xie, Y. Zhao, W. Lu and D. Li, Orthogonal-array dynamic molecular sieving of propylene/propane mixtures, *Nature*, 2021, **595**, 542-548.
13. P. C. Purba, M. Maity, S. Bhattacharyya and P. S. Mukherjee, A Self-Assembled Palladium(II) Barrel for Binding of Fullerenes and Photosensitization Ability of the Fullerene-Encapsulated Barrel, *Angew. Chem. Int. Ed.*, 2021, **60**, 14109-14116.
14. C.-X. Chen, Z.-W. Wei, T. Pham, P. C. Lan, L. Zhang, K. A. Forrest, S. Chen, A. M. Al-Enizi, A. Nafady, C.-Y. Su and S. Ma, Nanospace Engineering of Metal–Organic Frameworks through Dynamic Spacer Installation of Multifunctionalities for Efficient Separation of Ethane from Ethane/Ethylene Mixtures, *Angew. Chem. Int. Ed.*, 2021, **60**, 9680-9685.
15. L. Adriaenssens and P. Ballester, Hydrogen bonded supramolecular capsules with functionalized interiors: the controlled orientation of included guests, *Chem. Soc. Rev.*, 2013, **42**, 3261-3277.
16. D. Ajami, L. Liu and J. Rebek Jr, Soft templates in encapsulation complexes, *Chem. Soc. Rev.*, 2015, **44**, 490-499.
17. T. R. Cook, Y.-R. Zheng and P. J. Stang, Metal–Organic Frameworks and Self-Assembled Supramolecular Coordination Complexes: Comparing and Contrasting the Design, Synthesis, and Functionality of Metal–Organic Materials, *Chem. Rev.*, 2013, **113**, 734-777.
18. D. Zhang, T. K. Ronson and J. R. Nitschke, Functional Capsules via Subcomponent Self-Assembly, *Acc. Chem. Res.*, 2018, **51**, 2423-2436.
19. Y. Sun, C. Chen, J. Liu and P. J. Stang, Recent developments in the construction and applications of platinum-based metallacycles and metallacages via coordination, *Chem. Soc. Rev.*, 2020, **49**, 3889-3919.
20. E. G. Percástegui, T. K. Ronson and J. R. Nitschke, Design and Applications of Water-Soluble Coordination Cages, *Chem. Rev.*, 2020, **120**, 13480-13544.
21. M. Mastalerz, Porous Shape-Persistent Organic Cage Compounds of Different Size, Geometry, and Function, *Acc. Chem. Res.*, 2018, **51**, 2411-2422.
22. K. Acharyya and P. S. Mukherjee, Organic Imine Cages: Molecular Marriage and Applications, *Angew. Chem. Int. Ed.*, 2019, **58**, 8640-8653.
23. C. M. Hong, R. G. Bergman, K. N. Raymond and F. D. Toste, Self-Assembled Tetrahedral Hosts as Supramolecular Catalysts, *Acc. Chem. Res.*, 2018, **51**, 2447-2455.
24. C. T. McTernan, J. A. Davies and J. R. Nitschke, Beyond Platonic: How to Build Metal-Organic Polyhedra Capable of Binding Low-Symmetry, Information-Rich Molecular Cargoes, *Chem. Rev.*, 2022, **122**, 10393-10437.
25. J. Zhao, Z. Zhou, G. Li, P. J. Stang and X. Yan, Light-emitting self-assembled metallacages, *Natl. Sci. Rev.*, 2021, **8**, nwab045.
26. E. Sánchez-González, M. Y. Tsang, J. Troyano, G. A. Craig and S. Furukawa, Assembling metal-organic cages as porous materials, *Chem. Soc. Rev.*, 2022, **51**, 4876-4889.
27. Y. Domoto and M. Fujita, Self-assembly of nanostructures with high complexity based on metal unsaturated-bond coordination, *Coord. Chem. Rev.*, 2022, **466**, 214605.
28. M. Chen, J. Wang, D. Liu, Z. Jiang, Q. Liu, T. Wu, H. Liu, W. Yu, J. Yan and P. Wang, Highly Stable Spherical Metallo-Capsule from a Branched Hexapodal Terpyridine and Its Self-Assembled Berry-type Nanostructure, *J. Am. Chem. Soc.*, 2018, **140**, 2555-2561.
29. X. Yan, T. R. Cook, P. Wang, F. Huang and P. J. Stang, Highly emissive platinum(II) metallacages, *Nat. Chem.*, 2015, **7**, 342-348.
30. M. Han, R. Michel, B. He, Y.-S. Chen, D. Stalke, M. John and G. H. Clever, Light-Triggered Guest Uptake and Release by a Photochromic Coordination Cage, *Angew. Chem. Int. Ed.*, 2013, **52**, 1319-1323.
31. P. Mal, B. Breiner, K. Rissanen and J. R. Nitschke, White phosphorus is air-stable within a self-assembled tetrahedral capsule, *Science*, 2009, **324**, 1697-1699.
32. D. M. Kaphan, M. D. Levin, R. G. Bergman, K. N. Raymond and F. D. Toste, A supramolecular microenvironment strategy for transition metal catalysis, *Science*, 2015, **350**, 1235-1238.
33. P. P. Neelakandan, A. Jiménez, J. D. Thoburn and J. R. Nitschke, An Autocatalytic System of Photooxidation-Driven Substitution Reactions on a $Fe^{II}_4L_6$ Cage Framework, *Angew. Chem. Int. Ed.*, 2015, **54**, 14378-14382.
34. H. Takezawa, T. Kanda, H. Nanjo and M. Fujita, Site-Selective Functionalization of Linear Diterpenoids through U-Shaped Folding in a Confined Artificial Cavity, *J. Am. Chem. Soc.*, 2019, **141**, 5112-5115.
35. M. Morimoto, W. Cao, R. G. Bergman, K. N. Raymond and F. D. Toste, Chemoselective and Site-Selective Reductions Catalyzed by a Supramolecular Host and a Pyridine-Borane Cofactor, *J. Am. Chem. Soc.*, 2021, **143**, 2108-2114.
36. S. K. Samanta, D. Moncelet, V. Briken and L. Isaacs, Metal–Organic Polyhedron Capped with Cucurbit[8]uril Delivers Doxorubicin to Cancer Cells, *J. Am. Chem. Soc.*, 2016, **138**, 14488-14496.
37. B. Therrien, G. Süss-Fink, P. Govindaswamy, A. K. Renfrew and P. J. Dyson, The “ Complex-in-a-Complex ” Cations $[(Acac)_2M\subset Ru_6(P\text{-}iPrC_6H_4Me)_6(tpt)_2(dhbq)_3]^{6+}$: A Trojan Horse for Cancer Cells, *Angew. Chem. Int. Ed.*, 2008, **47**, 3773-3776.
38. Z. Ma and B. Moulton, Recent advances of discrete coordination complexes and coordination polymers in drug delivery, *Coord. Chem. Rev.*, 2011, **255**, 1623-1641.
39. N. Singh, J.-H. Jo, Y. H. Song, H. Kim, D. Kim, M. S. Lah and K.-W. Chi, Coordination-driven self-assembly of an iridium-cornered prismatic cage and encapsulation of three heteroguests in its large cavity, *Chem. Commun.*, 2015, **51**, 4492-4495.

40. S. Fujii, T. Tada, Y. Komoto, T. Osuga, T. Murase, M. Fujita and M. Kiguchi, Rectifying Electron-Transport Properties through Stacks of Aromatic Molecules Inserted into a Self-Assembled Cage, *J. Am. Chem. Soc.*, 2015, **137**, 5939-5947.
41. P.-F. Cui, X.-R. Liu, Y.-J. Lin, Z.-H. Li and G.-X. Jin, Highly Selective Separation of Benzene and Cyclohexane in a Spatially Confined Carborane Metallacage, *J. Am. Chem. Soc.*, 2022, **144**, 6558-6565.
42. Y. Wang, B. Li, J. Zhu, W. Zhang, B. Zheng, W. Zhao, J. Tang, X.-J. Yang and B. Wu, Light-Triggered High-Affinity Binding of Tetramethylammonium over Potassium Ions by [18]crown-6 in a Tetrahedral Anion Cage, *Angew. Chem. Int. Ed.*, 2022, **61**, e202201789.
43. R.-R. Liang, S.-Y. Jiang, R.-H. A and X. Zhao, Two-dimensional covalent organic frameworks with hierarchical porosity, *Chem. Soc. Rev.*, 2020, **49**, 3920-3951.
44. D. Luo, X. P. Zhou and D. Li, Beyond molecules: mesoporous supramolecular frameworks self-assembled from coordination cages and inorganic anions, *Angew. Chem. Int. Ed.*, 2015, **54**, 6190-6195.
45. Y. Kim, J. Koo, I. C. Hwang, R. D. Mukhopadhyay, S. Hong, J. Yoo, A. A. Dar, I. Kim, D. Moon, T. J. Shin, Y. H. Ko and K. Kim, Rational Design and Construction of Hierarchical Superstructures Using Shape-Persistent Organic Cages: Porphyrin Box-Based Metallosupramolecular Assemblies, *J. Am. Chem. Soc.*, 2018, **140**, 14547-14551.
46. G. L. Li, Z. Zhuo, B. Wang, X. L. Cao, H. F. Su, W. Wang, Y. G. Huang and M. Hong, Constructing π-Stacked Supramolecular Cage Based Hierarchical Self-Assemblies via π...π Stacking and Hydrogen Bonding, *J. Am. Chem. Soc.*, 2021, **143**, 10920-10929.
47. S. Chakraborty and G. R. Newkome, Terpyridine-Based Metallosupramolecular Constructs: Tailored Monomers to Precise 2D-Motifs and 3D-Metallocages, *Chem. Soc. Rev.*, 2018, **47**, 3991-4016.
48. Z. Gao, Y. Han, Z. Gao and F. Wang, Multicomponent Assembled Systems Based on Platinum(II) Terpyridine Complexes, *Acc. Chem. Res.*, 2018, **51**, 2719-2729.
49. D. Liu, K. Li, M. Chen, T. Zhang, Z. Li, J.-F. Yin, L. He, J. Wang, P. Yin, Y.-T. Chan and P. Wang, Russian-Doll-Like Molecular Cubes, *J. Am. Chem. Soc.*, 2021, **143**, 2537-2544.
50. R. H. Mitchell, V. S. Iyer, N. Khalifa, R. Mahadevan, S. Venugopalan, S. A. Weerawarna and P. Zhou, An Experimental Estimation of Aromaticity Relative to That of Benzene. The Synthesis and NMR Properties of a Series of Highly Annelated Dimethyldihydropyrenes: Bridged Benzannulenes, *J. Am. Chem. Soc.*, 1995, **117**, 1514-1532.
51. W. H. Miles, M. J. Robinson, S. G. Lessard and D. M. Thamattoor, Through-Space Shielding Effects of Metal-Complexed Phenyl Rings, *J. Org. Chem.*, 2016, **81**, 10791-10801.
52. T. Wu, Z. Jiang, Q. Bai, Y. Li, S. Mao, H. Yu, L. Wojtas, Z. Tang, M. Chen, Z. Zhang, T.-Z. Xie, M. Wang, X. Li and P. Wang, Supramolecular triangular orthobicupola: Self-assembly of a giant Johnson solid J27, *Chem*, 2021, **7**, 2429-2441.
53. T. Z. Xie, K. Guo, Z. Guo, W. Y. Gao, L. Wojtas, G. H. Ning, M. Huang, X. Lu, J. Y. Li, S. Y. Liao, Y. S. Chen, C. N. Moorefield, M. J. Saunders, S. Z. Cheng, C. Wesdemiotis and G. R. Newkome, Precise Molecular Fission and Fusion: Quantitative Self-Assembly and Chemistry of a Metallo-Cuboctahedron, *Angew. Chem. Int. Ed.*, 2015, **54**, 9224-9229.
54. S. Chakraborty, K. J. Endres, R. Bera, L. Wojtas, C. N. Moorefield, M. J. Saunders, N. Das, C. Wesdemiotis and G. R. Newkome, Concentration dependent supramolecular interconversions of triptycene-based cubic, prismatic, and tetrahedral structures, *Dalton Trans.*, 2018, **47**, 14189-14194.
55. S. Chakraborty, W. Hong, K. J. Endres, T. Z. Xie, L. Wojtas, C. N. Moorefield, C. Wesdemiotis and G. R. Newkome, Terpyridine-Based, Flexible Tripods: From a Highly Symmetric Nanosphere to Temperature-Dependent, Irreversible, 3D Isomeric Macromolecular Nanocages, *J. Am. Chem. Soc.*, 2017, **139**, 3012-3020.
56. M. Wang, R. Dong and X. Feng, Two-dimensional conjugated metal-organic frameworks (2D c-MOFs): chemistry and function for MOFtronics, *Chem. Soc. Rev.*, 2021, **50**, 2764-2793.
57. W. Wang, W. Zhao, H. Xu, S. Liu, W. Huang and Q. Zhao, Fabrication of ultra-thin 2D covalent organic framework nanosheets and their application in functional electronic devices, *Coord. Chem. Rev.*, 2021, **429**, 213616.
58. X. Zhao, P. Pachfule and A. Thomas, Covalent organic frameworks (COFs) for electrochemical applications, *Chem. Soc. Rev.*, 2021, **50**, 6871-6913.
59. A. Dhakshinamoorthy, A. M. Asiri and H. Garcia, 2D Metal-Organic Frameworks as Multifunctional Materials in Heterogeneous Catalysis and Electro/Photocatalysis, *Adv. Mater.*, 2019, **31**, 1900617.
60. J. Li, X. Jing, Q. Li, S. Li, X. Gao, X. Feng and B. Wang, Bulk COFs and COF nanosheets for electrochemical energy storage and conversion, *Chem. Soc. Rev.*, 2020, **49**, 3565-3604.
61. X. Cai, Y. Luo, B. Liu and H.-M. Cheng, Preparation of 2D material dispersions and their applications, *Chem. Soc. Rev.*, 2018, **47**, 6224-6266.
62. C. Zhang, B.-H. Wu, M.-Q. Ma, Z. Wang and Z.-K. Xu, Ultrathin metal/covalent-organic framework membranes towards ultimate separation, *Chem. Soc. Rev.*, 2019, **48**, 3811-3841.
63. R.-B. Lin, S. Xiang, H. Xing, W. Zhou and B. Chen, Exploration of porous metal-organic frameworks for gas separation and purification, *Coord. Chem. Rev.*, 2019, **378**, 87-103.
64. D. Wu, P.-F. Zhang, G.-P. Yang, L. Hou, W.-Y. Zhang, Y.-F. Han, P. Liu and Y.-Y. Wang, Supramolecular control of MOF pore properties for the tailored guest adsorption/separation applications, *Coord. Chem. Rev.*, 2021, **434**, 213709.
65. J. Wang and S. Zhuang, Covalent organic frameworks (COFs) for environmental applications, *Coord. Chem. Rev.*, 2019, **400**, 213046.
66. Y. Li, Z. Li, C. Chi, H. Shan, L. Zheng and Z. Fang, Plasmonics of 2D Nanomaterials: Properties and Applications, *Adv. Sci.*, 2017, **4**, 1600430.
67. P. T. Speakman, Proposed Mechanism for the Biological Assembly of Collagen Triple Helix, *Nature*, 1971, **229**, 241-243.
68. D. R. Walker, S. A. H. Hulgan, C. M. Peterson, I. C. Li, K. J. Gonzalez and J. D. Hartgerink, Predicting the stability of homotrimeric and heterotrimeric collagen helices, *Nat. Chem.*, 2021, **13**, 260-269.
69. H. Wang, K. Wang, Y. Xu, W. Wang, S. Chen, M. Hart, L. Wojtas, L.-P. Zhou, L. Gan, X. Yan, Y. Li, J. Lee, X.-S. Ke, X.-Q. Wang, C.-W. Zhang, S. Zhou, T. Zhai, H.-B. Yang, M. Wang, J. He, Q.-F. Sun, B. Xu, Y. Jiao, P. J. Stang, J. L. Sessler and X. Li, Hierarchical Self-Assembly of Nanowires on the Surface by Metallo-Supramolecular Truncated Cuboctahedra, *J. Am. Chem. Soc.*, 2021, **143**, 5826-5835.
70. R. O. Erickson, Tubular Packing of Spheres in Biological Fine Structure, *Science*, 1973, **181**, 705-716.
71. R. Pawlak, X. Liu, S. Ninova, P. D'Astolfo, C. Drechsel, J.-C. Liu, R. Häner, S. Decurtins, U. Aschauer, S.-X. Liu and E. Meyer, On-Surface Synthesis of Nitrogen-Doped Kagome Graphene, *Angew. Chem. Int. Ed.*, 2021, **60**, 8370-8375.
72. Q. Hao, Z.-J. Li, B. Bai, X. Zhang, Y.-W. Zhong, L.-J. Wan and D. Wang, A Covalent Organic Framework Film for Three-State Near-Infrared Electrochromism and a Molecular Logic Gate, *Angew. Chem. Int. Ed.*, 2021, **60**, 12498-12503.